Performance of unbound pavement materials in changing moisture conditions

Marit Fladvad

Department of Geoscience and Petroleum, NTNU – Norwegian University of Science and Technology.

Norwegian Public Roads Administration. marit.fladvad@vegvesen.no

Sigurdur Erlingsson

Pavement Technology, Swedish National Road and Transport Research Institute (VTI). sigurdur.erlingsson@vti.se

Faculty of Civil and Environmental Engineering, University of Iceland

Abstract Expected climate changes will in many areas represent a shift towards increased precipitation and more intense rainfall events. This may lead to increased moisture within road structures and possible overloading of road drainage systems. Pavement design methods must therefore be able to predict the behaviour of pavement materials at increased moisture levels. An instrumented accelerated pavement test (APT) has been conducted on two thin flexible pavement structures with coarse-grained unbound base course and subbase materials using a heavy vehicle simulator (HVS). The two pavement structures were identical except for the grain size distribution of the subbase material, where one had a dense 0/90 mm curve with a controlled fines content, and the other had an open-graded 22/90 mm curve. The APT was conducted using constant dual wheel loading, and three different groundwater levels were induced in order to change the moisture content in the structures. The HVS was stopped regularly for carrying out response measurements from the instrumentation. The analysis is focussed on the response and the performance of the unbound aggregate layers to varying moisture levels in the pavement structure.

Keywords Accelerated pavement test; heavy vehicle simulator; moisture content; groundwater table.

1 Introduction

Environmental conditions are important inputs to pavement design, combined with traffic load, material choice and layer thicknesses. Pavement design has traditionally been done using empirical methods, based on long-term experience with similar materials and conditions (ARA Inc., 2004). When climate changes cause a shift towards increased precipitation and more intense rainfall events, empirical methods can no longer be used to predict pavement performance. A transition from empirical to mechanistic design is needed, and to achieve this, we need to be able to model the behaviour of the pavement structures under all conditions (Erlingsson, 2007).

In the Nordic countries, most roads are designed using flexible pavements, with relatively thin hot mix asphalt (HMA) layers above thicker unbound base and subbase providing a substantial part of the bearing capacity. This practice is partly due to the availability of high-quality aggregate resources, making unbound aggregates an affordable solution.

In Norway, local aggregate resources originating from tunnels and road cuts are often utilized in construction projects. Aggregates can be produced and used on-site, reducing transportation costs for raw materials. Due to space and time restrictions at the construction sites, such production requires a simple setup. These restrictions, combined with experience with frost heave problems caused by excess fines, have resulted in a practice where all fine material is sorted out from the large-size aggregate used in the subbase layer (Aarstad et al., 2019; Aksnes et al., 2013).

In Sweden, on the other hand, aggregate resources are normally transported in from quarries where the production methods allow for full quality assessment of the products. Here, large-size aggregate materials with controlled fines content are used in the subbase layer.

Water and moisture have a large influence on the performance of pavement materials (Dawson, 2009). As the moisture content increases, the friction between aggregate particles becomes lower, and the resistance to differential particle deformation is reduced, leading to a reduced resilient modulus of unbound aggregates (ARA Inc., 2004; Erlingsson, 2010; Lekarp and Dawson, 1998).

The main objective of the current research is to examine the effect of gradation on the performance of subbase materials when tested at three different groundwater levels. Two subbase materials of equal geological composition are tested, one material containing fines, while all particles < 22 mm were removed from the other material. Albeit being composed of the same rock type, such materials will have different properties regarding density, void ratio, permeability and stiffness. Depending on gradation, varying groundwater levels result in varying moisture content in the pavement materials also above the groundwater table (GWT); hence, the influence of moisture content on pavement performance can be evaluated (Erlingsson, 2010; Li and Baus, 2005; Saevarsdottir and Erlingsson, 2013).

In order to examine the effects in full scale, an accelerated pavement test (APT) using a heavy vehicle simulator (HVS) was chosen. The APT was conducted at the Swedish National Road and Transport Research Institute (VTI) test facility in Linköping, Sweden in 2018-2019.

2 Materials and methods

The APT was conducted using an HVS at the VTI full-scale pavement testing facility. The pavement structures were constructed in a concrete test pit which is 3 m deep, 5 m wide and 15 m long. In the test pit, GWT can be controlled and adjusted.

2.1 Pavement structure

Two pavement structures were tested simultaneously in order to investigate the difference between an open-graded and a well-graded subbase. The subbase gradations 0/90 mm and 22/90 mm were chosen; otherwise, the two pavement structures were constructed of identical materials.

The surface course and bituminous base course was constructed from asphalt concrete (AC) with upper aggregate size 16 and 22 mm, respectively. Base course (0/32 mm) and subbase were constructed from unbound crushed rock. The subgrade consisted of silty sand. Layer thicknesses for the pavement structures are shown in Fig. 1. The difference in layer thicknesses between the two structures is due to practical adjustments in the construction process, such as differences in compaction.

The subbase materials are supplied from a tunnel construction site in the construction project E39 Svegatjørn–Rådal south of Bergen, Norway. The materials fulfil requirements for subbase materials regarding gradation, fines content and physical properties (Norwegian Public Roads Administration, 2018). The open-graded material was selected from the ongoing production at the construction site, while the well-graded material was created by mixing 22/90 and 0/32 mm material 1:1 by weight.

2.2 Accelerated pavement test

The HVS was set up with a dual-wheel configuration; the dual-wheel load during testing was 60 kN, corresponding to 120 kN axle load. The tyre pressure was 800 kPa, and the wheel spacing was 34 cm centre-to-centre. The lateral wander of the

wheel was ±25 cm in 5 cm increments, following a normal distribution curve. The rolling wheel speed was 12 km/h, and the temperature was held constant at 10ºC by use of a climate chamber. The initial 20 000 load repetitions were conducted as a pre-loading phase with lower load (30 kN) and even lateral distribution in order to post-compact the structures.

Both pavement structures were instrumented using asphalt strain gauges (ASG), soil pressure cells (SPC), strain measuring units (εMU) and moisture sensors (Fig. 1). Additionally, the surface rut profile was measured using a laser and straight edge setup. The instrumentation is described in detail by Saevarsdottir et al. (2016), who used the same test facility and similar equipment.

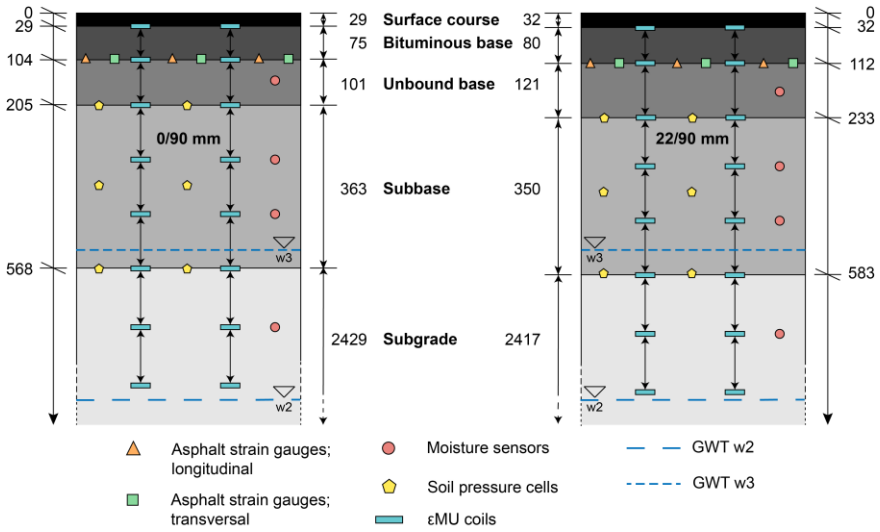

Fig. 1 Cross section of the pavement structures, including position of sensors. Layer thickness and depth below surface measured in mm. The GWT for phase w1 was located > 3 m below the surface. Horizontal distance between sensors not to scale

ASGs measure the longitudinal and transversal strain at the bottom of the AC layers. SPCs measuring vertical stress are distributed at the top, middle and bottom of the subbase. εMUs measure vertical strain at 7 different levels; over the bound base layer, unbound base layer, three levels in the subbase and two levels in the subgrade, the lowest reaching to approximately 30 cm below the formation level. Moisture content was measured at four different levels; in the subgrade approximately 15 cm below the formation level, at two levels in the subbase layer, and in the middle of the base layer. The pavement response was measured at regular intervals during the test. Measurements using falling weight deflectometer (FWD) was conducted in each phase. FWD measurements were conducted before the accelerated traffic started and at the end of phase w2 and w3.

2.3 Groundwater table

The APT was divided into three phases, each with a separate depth of the GWT. In phase w1, GWT was located at great depth, > 3 m below the pavement surface. GWT was stable at this level for the first 550 000 load repetitions. For phase w2, GWT was raised to 30 cm below the formation level, corresponding to the depth of the drainage level of a pavement structure in operation. GWT was stable at this level for 368 000 load repetitions. For phase w3, GWT was raised further to a level of about 5 cm above the formation level. This level simulates a situation where the drainage system is overloaded and unable to keep the GWT at the designed drainage level. GWT was stable at this level for 286 000 load repetitions. No traffic load was applied while GWT was raised.

3 Results

3.1 Water content

Table 1 shows the volumetric water content for all three phases. The water content in the subgrade increases from 12.8 % to 27.7 %, corresponding to full saturation. The 0/90 mm subbase and overlying base show an increase in water content when GWT is introduced in the subgrade. For the open-graded structure, it is only at the end of phase w3 that an increase in water content is visible in the base course.

Table 1 Volumetric water content in unbound base, subbase and subgrade at the time of FWD measurements

	0/90 mm structure			22/90 mm structure		
	w1	w2	w3	w1	w2	w3
Base course	7.7 %	8.6 %	10.0 %	7.1 %	7.2 %	10.0 %
Upper subbase	6.1 %	6.5 %	6.7 %	2.1 %	2.2 %	2.5 %
Lower subbase	8.6 %	9.2 %	10.2 %	1.5 %	1.6 %	2.1 %
Subgrade	12.8 %	26.6 %	27.7 %	12.8 %	26.6 %	27.7 %

3.2 FWD back-calculation

FWD measurements were conducted at all three GWT levels. Table 2 shows the back-calculated stiffness moduli for each phase. As the climate chamber had to be removed in order to enable FWD measurements, the temperature could not be

controlled at 10ºC for these measurements. To allow the comparison of deflection bowls in Fig. 2, the FWD results have been back-calculated with the resilient modulus for the AC layers adjusted corresponding to 10°C. In the back-calculation procedure, the subbase was divided into three sublayers and the subgrade into two layers.

The 22/90 mm structure has the highest deflection in phase w1, but is less affected by the raised GWT in phases w2 and w3, compared to the 0/90 mm structure. From the stiffness values, it appears that the difference in deflection between phase w1 and w2 in the 22/90 mm structure is only due to the decrease in subgrade stiffness. For the 0/90 mm structure, on the other hand, base and subbase stiffness is also affected by the introduction of a GWT in phase w2. Between phase w2 and w3, stiffness in all layers is affected. The reduced AC stiffness is not directly related to the increased GWT, but a result of pavement degradation due to the 1.2 million load repetitions.

Table 2 Back-calculated resilient moduli at 10°C in the pavement structure at the three groundwater levels

	0/90 mm structure				22/90 mm structure			
	Thickness [mm]	Stiffness modulus [MPa]			Thickness [mm]	Stiffness modulus [MPa]		
		w1	w2	w3		w1	w2	w3
AC layers	104	6500	6500	5671	112	6500	6500	5671
Unbound base	101	250	225	203	121	250	250	203
Subbase 1	163	220	157	149	150	143	143	135
Subbase 2	150	220	143	129	150	143	143	135
Subbase 3	50	220	129	116	50	143	143	135
Subgrade 1	300	82	66	46	300	82	66	46
Subgrade 2	2132	82	53	46	2117	82	53	46

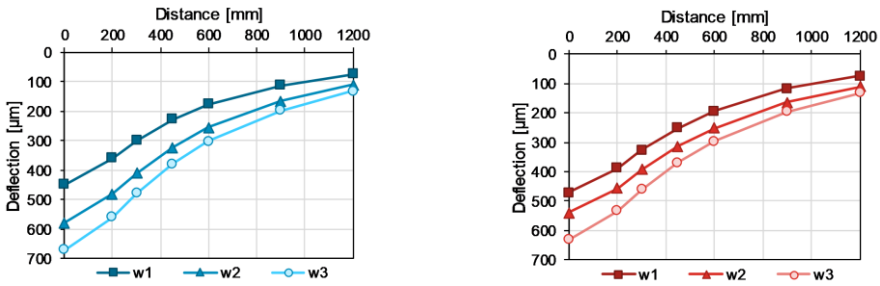

a) 0/90 mm structure b) 22/90 mm structure

Fig. 2 Adjusted deflection bowl based on back-calculated stiffness parameters from FWD measurements with load 50 kN at 10°C

3.3 Stress

Fig. 3 shows the typical registration of an SPC. Four consecutive registrations as the wheel load pass over the sensor are shown after 377 000, 555 000 and 940 000 load repetitions. The effect of the change in moisture content in the three phases (w1, w2 and w3) is evident as the measured stress decreases significantly between the phases.

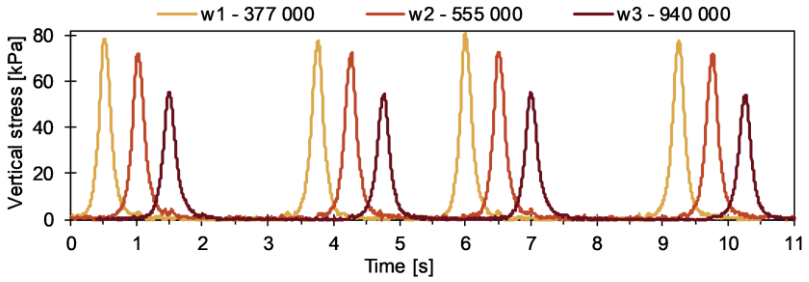

Fig. 3 Vertical stress signals registered at a sensor located in the middle of the subbase layer of the 0/90 mm structure after 377 000 (w1), 555 000 (w2) and 940 000 (w3) load repetitions

Fig. 4 shows the development of measured stress throughout the APT. A post-compaction effect is seen in phase w1, as the stress increases gradually. The stress decreases after each GWT raise, before it increases toward the end of the test.

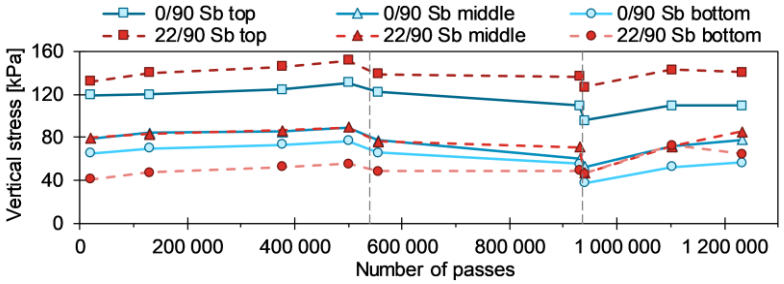

Fig. 4 Development of measured vertical stress at three levels in the two subbase layers. Vertical dashed lines indicate GWT raise. Initial measurement made after 20 000 load repetitions.

3.4 Strain

The measured vertical strain at three levels in the subbase layer is displayed in Fig. 5. The strain increases throughout each phase, while it decreases at each GWT raise. The decrease in measured strain as GWT was raised was not ex-

pected. This indicates that the structure is getting stiffer, which disagrees with the SPC registrations in Fig. 3 and Fig. 4, as well as the FWD measurements. Response measurements using 50 kN wheel load was also analysed, and showed the exact same tendency for both stress and strain as Fig. 4 and Fig. 5.
Registered strain signals from two sensors in the lower part of the subbase layers are displayed in Fig. 6. No difference in strain is visible between phases w1 and w2, while in phase w3, strain increases by 60-70 %.

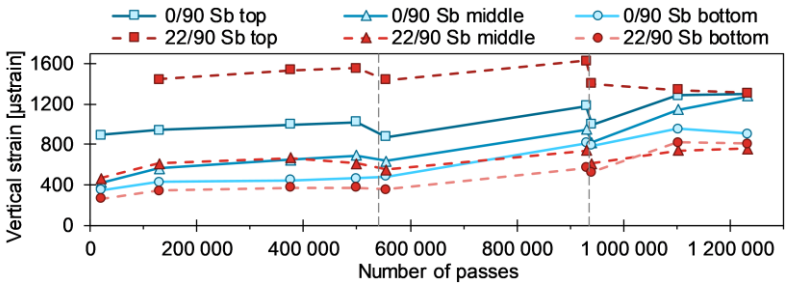

Fig. 5 Development of measured vertical strain at three levels in the two subbase layers. Vertical dashed lines indicate GWT raise. Initial measurement made after 20 000 load repetitions.

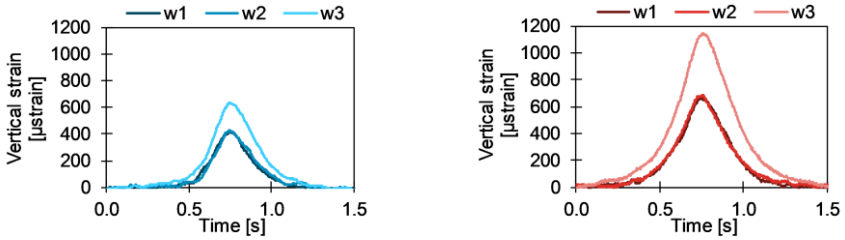

a) 0/90 mm structure **b)** 22/90 mm structure

Fig. 6 Vertical strain measured in the lowest part of the subbase layer after 377 000 (w1), 555 000 (w2) and 940 000 (w3) load repetitions

3.5 Rut development

The surface rut development during the APT is shown in Fig. 7. A post-compaction tendency can be observed from the increased rut development for the initial 20 000–30 000 load repetitions. The 0/90 mm structure obtains a surface rut depth of 19.9±1.0 mm after 1 233 000 load repetitions, compared to 20.3±0.7 mm for the 22/90 mm structure.
The average rate of rut for each phase is calculated in Table 3. The rate of rut increases for each GWT raise.

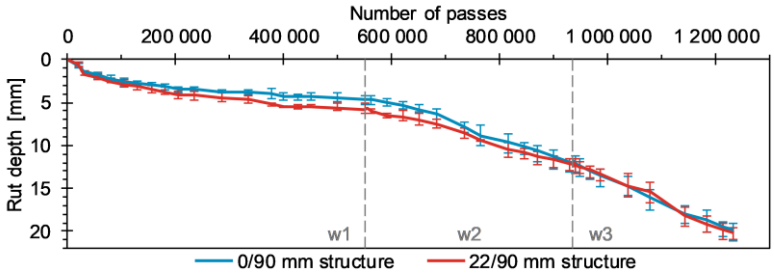

Fig. 7 Rut development during APT. Each line represents the average of three laser profiles; error bars show max/min measurements. Dashed vertical lines indicate GWT phase transitions

Table 3 Average rut rate the last ≈200 000 load repetitions of each phase [mm per 100 000 load repetitions]

	w1	w2	w3
0/90 mm structure	0.43	2.14	2.67
22/90 mm structure	0.56	1.78	2.80

4 Conclusions

Two instrumented flexible pavement structures were tested by an HVS where the GWT table was increased twice during the APT. Moisture, stresses and strains in the pavement were measured, along with surface deflection from FWD and rut depth.

Both pavement structures proved to be durable, showing about 20 mm rut depth after 1.2 million load repetitions with a 60 kN dual-wheel load (axle load 12 tonnes). The accelerated traffic corresponds to 2.55 million 10 tonne standard axles or an annual average daily traffic of about 3000 vehicles per day over 20 years, assuming the amount of heavy vehicles is 10 %.

Pavement response and rut development are affected by the GWT level. When the GWT is raised, SPC register lower stress levels; hence, the stiffness is decreased. The vertical strain measurements indicate a decrease in strain as GWT is raised, indicating that the stiffness of the pavement materials increases. This is not in agreement with SPC or FWD measurements. The authors are unable to explain this effect, and these results must be studied further.

The rutting accelerates considerably as GWT is introduced to the upper part of the structure. Even though the structures respond differently to the GWT increases, both reach a maximum rut rate of about 2.7 mm per 100 000 load repetitions in phase w3, and similar rut depth when the test is finished.

For both structures, flooding results in a substantial increase in pavement degradation. The data provided from the APT presented here can be used to model

unbound materials' response to increased moisture content following increased precipitation and more intense rainfall events.

Acknowledgements This research is funded by the Norwegian Public Roads Administration, with contribution from the Research Council of Norway (project no. 256541). The manuscript is a part of the first author's PhD degree at NTNU. The authors would like to thank Veidekke for supplying the subbase materials to the APT.

References

Aarstad K, Petersen BG, Martinez CR et al (2019) Local use of rock materials - production and utilization. State-of-the-art. SINTEF, Trondheim,. https://www.sintef.no/globalassets/project/kortreist-stein/012-kortreist-stein-sota-h3-endelig.pdf

Aksnes J, Myhre Ø, Lindland T et al (2013) Frost protection of Norwegian Roads. Basis for revision of the Norwegian pavement design manual, Statens vegvesens rapporter nr. 338. Norwegian Public Roads Administration, Trondheim. https://www.vegvesen.no/fag/publikasjoner/publikasjoner/statens+vegvesens+rapporter/_attachment/748672?_ts=14a524bccb8

ARA Inc. (2004) Guide for the Mechanistic-Empirical Design of New and Rehabilitated Pavement Structures, Final report, NCHRP 1-37A. Washington DC.

Dawson A (ed) (2009) Water in Road Structures - Movement, Drainage & Effects. Springer Netherlands, Dordrecht. doi:10.1007/978-1-4020-8562-8

Erlingsson S (2010) Impact of Water on the Response and Performance of a Pavement Structure in an Accelerated Test. Road Mater Pavement Des 11:863-880. doi:10.1080/14680629.2010.9690310

Erlingsson S (2007) Numerical Modelling of Thin Pavements Behaviour in Accelerated HVS Tests. Road Mater Pavement Des 8:719-744. doi:10.1080/14680629.2007.9690096

Lekarp F, Dawson A (1998) Modelling permanent deformation behaviour of unbound granular materials. Constr Build Mater 12:9-18. doi:10.1016/S0950-0618(97)00078-0

Li T, Baus RL (2005) Nonlinear Parameters for Granular Base Materials from Plate Tests. J Geotech Geoenvironmental Eng 131:907-913. doi:10.1061/(ASCE)1090-0241(2005)131:7(907)

Norwegian Public Roads Administration (2018). Håndbok N200 Vegbygging. Statens vegvesen Vegdirektoratet, Oslo. https://www.vegvesen.no/_attachment/2364236/binary/1269980

Saevarsdottir T, Erlingsson S (2013) Water impact on the behaviour of flexible pavement structures in an accelerated test. Road Mater Pavement Des 14:256-277. doi:10.1080/14680629.2013.779308

Saevarsdottir T, Erlingsson S, Carlsson H (2016) Instrumentation and performance modelling of heavy vehicle simulator tests. Int J Pavement Eng 17:148-165. doi:10.1080/10298436.2014.972957